

Low-Cost Optoelectronic Devices to Measure Velocity of Detonation

Edwin M. Chan^a, Vivian Lee^a, Samuel P. Mickan^a, Phil J. Davies^b

^aUniversity of Adelaide, North Tce., Adelaide, Australia 5005

^bDefence Science and Technology Organisation, Salisbury, Australia 5111

ABSTRACT

Velocity of Detonation (VoD) is an important measured characteristic parameter of explosive materials. When new explosives are developed, their VoD must be determined. Devices used to measure VoD are always destroyed in the process, however replacing these devices represents a considerable cost in the characterisation of new explosives. This paper reports the design and performance of three low-cost implementations of a point-to-point VoD measurement system, two using optical fibre and a third using piezoelectric polymers (PolyVinylidene Fluoride, PVDF). The devices were designed for short charges used under controlled laboratory conditions and were tested using the common explosive 'Composition B'. These new devices are a fraction of the cost of currently available VoD sensors and show promise in achieving comparable accuracy. Their future development will dramatically reduce the cost of testing and aid the characterisation of new explosives.

Keywords: Explosions, Shock waves, Optical velocity measurement, Piezoelectric devices

1. INTRODUCTION

The evaluation of new explosive compounds is an important part of their development. Velocity of Detonation (VoD) measurement forms a part of the suite of tests which are used to characterise these explosives [5]. VoD is the speed at which the detonation front propagates down the length of the explosive. In the detonation of high explosives, the energy for the reaction is supplied by a supersonic shockwave which compresses the material [12]. This is different from combustion where the energy is supplied by heat transfer. The reaction of High Explosive (HE) material itself produces a shockwave which sustains and accelerates the speed of the shockfront until a balance is reached. Once this is reached, the VoD becomes constant.

The measurement of VoD relies on several different effects present at or near the shock front. Following the high pressure discontinuity of the shockfront is a region of ionised particles formed through the breaking of molecular bonds caused by the shock front. In the breaking of these bonds, as well as the reformation of stable molecules, light emission occurs. Hence pressure, ionisation and light can be used as indicators for the passage of the shock front.

Piezoelectric pins are an accepted means of measuring the VoD. They are currently used by the DSTO, and will be the method evaluated against. These pins are accurate, durable and easy to setup. However each pin costs \$30 and 10 are consumed per test. At least three destructive VoD tests need to be run per diameter to ensure statistical accuracy, equating to large testing costs. In this work, a cheap optical and piezo-based approach is reported for measuring constant VoD. They showed promising results and with future development are poised as a cheaper alternative to the piezoelectric pins currently employed by the DSTO.

2. MEASUREMENTS OF VOD

2.1 Determining Constant VoD

A constant VoD is achieved a short time after detonation of the HE. This constant VoD will be the parameter quoted for an explosive. It can be measured by both a continuous VoD measurement system and also simpler point-to-point VoD systems. A point to point VoD system is made up by a discrete number of sensors. These sensors are placed at known separations along the length-wise axis of the charge, as far from the start of detonation as feasible, when the speed of shockwave should have stabilised. By measuring the time it takes for the shockwave to travel from one sensor to the next, and knowing the separation distance, the average VoD can be calculated. This investigation looked at possible optical and piezo based realisation for these sensors.

2.2 Model of Light Generation

An established model for light generation due to shock waves suggests that the shockwave compresses the material/gas causing heating of the material [9]. This temperature increase results in light emission over a continuous spectrum at explosive temperatures. The high-temperature emission spectra resembles black body radiation, thus total radiated power,

$$P \propto T^4 \quad (1)$$

where T is temperature in Kelvin. The thermal luminosity further depends on the compressibility of the material [9]. A gas will reach a higher temperature and hence gives off more light because it is more compressible than, for example, a solid.

Assuming black body radiation, the power spectrum can be derived using Plank's Energy Distribution [2] [13],

$$P_\lambda = \frac{2\pi hc^2}{\lambda^5 \left(\exp\left(\frac{hc}{\lambda kt}\right) - 1 \right)} \quad (2)$$

and the light intensity at the shock front can be predicted. According to a DSTO detonation model, the temperature at the detonation front is about 4000K [7]. The distribution at this temperature is plotted in Fig. 1. Integrating under the graph of Plank's Energy Distribution for most of the sensitive region of the photodiode used (300nm to 1200nm) yields an estimated power density of at least 8.8MW/m², forming a maximum light intensity expected.

2.3 Piezoelectric Materials and Shock

There are numerous examples of work using piezoelectric materials to measure the pressures at the shockfront, such as [15]. Pioneering work into the use of PVDF sensors for shock and blast measurements were done by Bauer [6]. The basis of measuring the pressures at the shockfront is the piezoelectric effect. Piezoelectricity is the ability of certain crystals to become electrically polarised. That is, to produce a voltage when they undergo mechanical strain. Such materials are called piezoelectric materials. Piezoelectric materials are, at rest, electrically neutral like normal non-conducting materials. However as stress is applied to the material such as by a shock/force, the symmetry between the positive and negative charges in the crystals becomes unbalanced. The unbalancing of charges causes a polarisation in the material, which is directly proportional to the strain and the direction the force is applied. This polarisation is seen as a potential difference across the material which will vary proportionally to the magnitude of force being applied, hence magnitudes of pressure can be measured.

In the use of such materials the polarisation direction of a piezoelectric material is also very important and can be demonstrated by an example. Fig. 1 shows the position of the different charges when the material is at rest. Notice that the charges are arranged hexagonally. Consider now that force is applied along the x axes – the material is then compressed horizontally towards the centre where the three positive charges acting against the three negative charges to cancel out one another. Hence there is no potential difference along the x axes. However consider when the force is applied along the y axes. The material is compressed in such a way that there are now two positive charges on one end

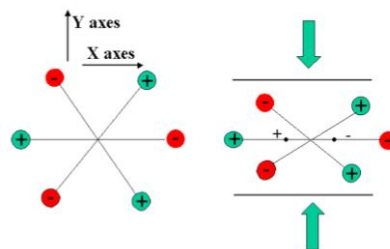


Figure 1: The two diagrams show the position of +ve and -ve charges in piezoelectric materials a) left: charges when materials is at rest, b) right: charges position when material is being stressed [11].

of the material and two negative charges on the other. This therefore forms a dipole and a potential difference exists along the x axes [11]. The example illustrates that it is important to align the piezo material in a way that ensures correct polarisation in order to obtain reasonable results. Previous work provided a good basis for showing feasibility however it remained uncertain what the shape of the response would be in the implementation chosen.

3. PROTOTYPE DESIGN

The device was separated into two parts, a sensor array and a sensor to oscilloscope interface circuit (Fig. 2). This interface circuit was a photo detector circuit for the optical prototypes and a buffer amplifier for the PVDF prototypes. The sensor array would be consumed in the test, while the interface circuitry would remain safely outside the blast chamber. By minimising the amount of material and equipment destroyed per test, the cost per test should be minimised.

Two main approaches were taken in the design of the device. From the basic concept these were built, tested, evaluated, and iteratively improved. This was the only realistic methodology given the not well understood or modelled detonation theory available. The most successful designs for each of the three approaches are shown in detail below.

3.1 Device A: Perpendicularly Mounted Fibres

This sensor consists of 1mm core Poly Methyl MethaAcrylate (PMMA) fibres held perpendicularly against the charge such that the tips of the fibre are in contact with the charge. Perpendicularity is important to ensure that any light picked up can be traced back to a particular area of the charge just below the sensor.

A drilled lateral segment of a PVC pipe of diameter larger than the charge under test was used to hold the fibres and maintain a known separation.

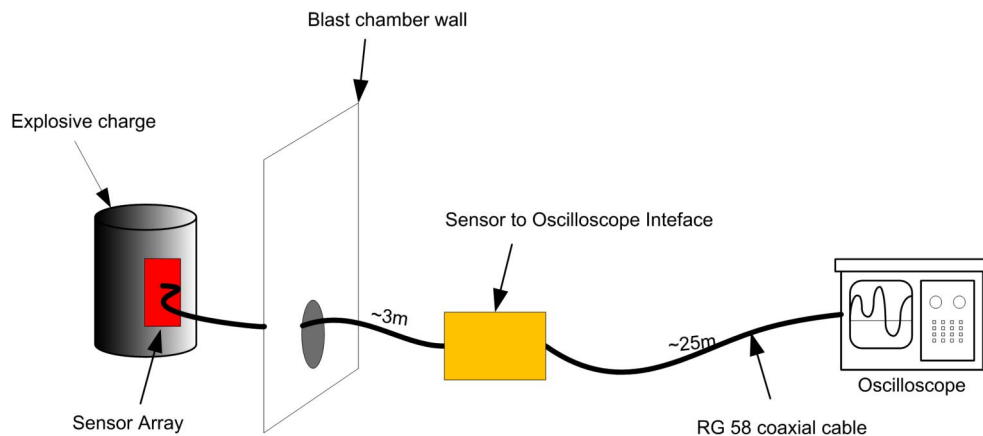


Figure 2: Modules of the proposed system which consists of a sensor array and photo detector circuit. Reducing the amount of equipment on the sensor array will reduce the cost incurred each test.

3.2 Device B: Fibre Optic Probe

The Fibre Optic Probe (FOP) consists of a single fibre in which several cavities are created. The air in these cavities is compressed by the shock wave, ionising the molecules in the air and emitting light. This technique was first suggested by [10] with all published current work being done by [4].

A ‘thick’ 1mm core cladded PMMA fibre was drilled with 0.5mm diameter holes, forming the cavities (Fig. 3). The cladding was left on the fibre to prevent light entering the fibre from other than the cavities. Furthermore, the end of the fibre next to the explosive is covered by melting the opaque cladding over the fibre face, also to prevent light entering from other than the cavities. Another method using a metal cap was also tried, however both gave similar results and these are presented together in the results. The fibre is positioned along the grooves a ribbon cable and glued. This helps

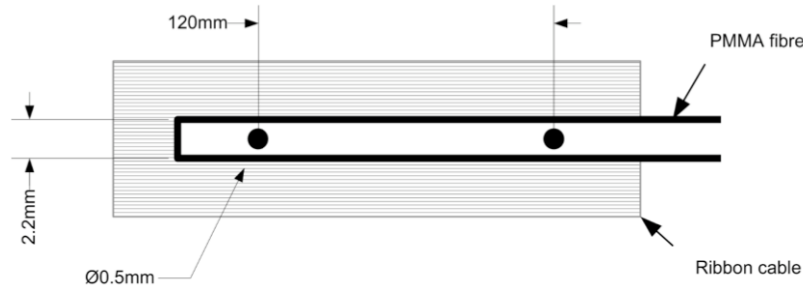


Figure 3: Schematic view of FOP, showing drilled cavities. A ribbon cable strengthens the sensor array and helps with the fibre alignment.

to stiffen and align the fibre, simplifying manufacture and providing a simple means to mount the sensors such that the cavities are directed towards the charge surface.

3.3 Photo-detector Circuit

A silicon PIN photo diode was chosen because of its low cost and relatively fast response. The photodiode was not biased, to simplify voltage supply requirements, and used with an op-amp based transimpedance amplifier [8]. The sensitivity of the photo-detector circuit is controlled by the feedback resistance. It was difficult to ‘design’ for a suitable maximum power of light because such a value is not well established and the losses at the various interfaces of the fibre were not well known. Instead, the value used was found through iterative testing. Theoretical simulations are possible to gauge the power density of the source which a fibre and photo-detector pair can cope with before saturation. However again without an accurate estimate of the losses as the light enters the fibre, and when it exits into the photodiode, such estimates may be inaccurate, up to a degree of several orders of magnitude.

Following this, a buffer output stage was required to drive a large capacitive load arising from the use of long coaxial cables. These cables connect the areas directly outside the blast chamber with the control room where measurements are recorded.

3.4 Device C: PVDF

The PVDF device sandwiches thin, short lengths of PVDF film between two PCB boards. The PVDF film consists of a layer of piezo polymer with metallic layers manufactured on both surfaces. This metallic layer provides a conductive surface from which to look at the potential difference which is generated across the piezo material. During preparation, cutting this film may press these layers together, short-circuiting the upper and lower electrodes. To prevent this, Acetone was used to remove some areas of the metallic coating. These cleaned sensors sit inside the PCBs such that metal tracks on the PCBs are in contact with opposite sides of the PVDF, which with consistent pressure provides the required electrical connection (Fig. 4). The boards are clamped and glued to maintain this connection.

Each sensor was recorded separately, with the sensor array connected to the sensor to oscilloscope interface via RG-58 coaxial cable. This connection was provided off the PCB through screw connectors on a small piece of Vero board with single strand wiring back to the PCBs. Having this off the PCB allowed the PCBs to sit flatter on the charge surface, placing the sensor closer to the surface. An additional 20 kΩ resistor was placed between the pair of lines attached to a single sensor to prevent the formation of high resistance paths when the piezo films were ‘at rest’ and acting as non-conductors. The outputs of these sensors were buffered outside the blast chamber using an op-amp based amplifier before going to the recording equipment some distance away.

4. CONSTRUCTION

4.1 Fibre to Photodiode Coupling

To facilitate easy and acceptably accurate positioning of the fibre with respect to the photodiode, a ‘cap’ was manufactured which would fit over the photo diode while holding the fibre straight and centred over the active element of the photodiode. The manufacture and use of this cap is shown in Fig. 5.

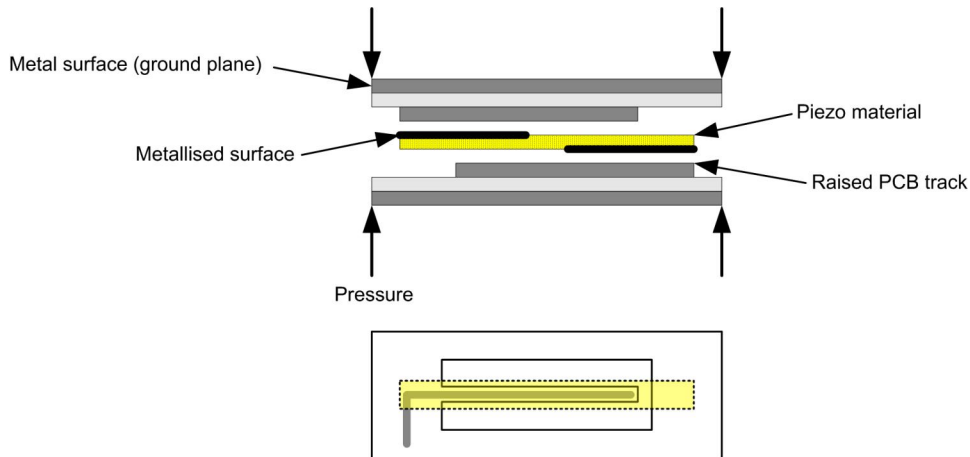


Figure 4: Schematic view of PVDF film being sandwiched between two PCB boards. The metallic layers of the PVDF film have been removed to eliminate possible short circuiting.

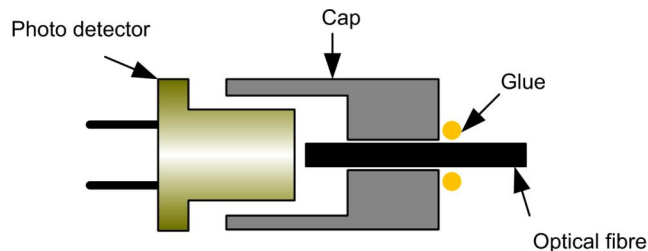


Figure 5: A schematic view of how the 'cap' holds, and aligns the optical fibres over the central axis of the photo diode. This was a cheap method of ensuring quick to use, but adequate coupling between the fibre and the diode.

The cap was readily manufactured from a commercially produced tapped nylon spacer, which is normally used to secure and elevate a PCB from a surface. This nylon spacer is drilled out to the appropriate diameter on one end to fit the photodiode. The fibre could then be fitted through the other end, or if a thinner fibre than the internal diameter of the nut was used, the hole could be drilled into a fitting plastic screw which could then be screwed in the nut.

4.2 Enclosure

The circuits were housed in a grounded steel box to shield the components from external EM interference. Power and signal connections to the circuit boards are made via header pins and removable sockets to allow easy repair and replacement of the circuitry. Power is brought into the box via the visible panel mount socket, and the output signal taken out via BNC socket mounts. Holes just sufficient for the "connectors" on ends of the fibre optic cables were drilled in close proximity to where the photo detector would sit inside the box to facilitate connection of the fibre to the photo diode. The effect of the holes in the box allowing high frequency interference to enter the box was not considered a serious design problem. Testing showed that this was not an issue, and could always be rectified using foil while on site.

5. TESTING

5.1 Explosive Test Setup

The devices were tested on similar setups. The explosive train consisted of a detonator, booster and main charge. The main charges were either 485g or 550g of (60/40 RDX/TNT) Composition B. The explosive was cast and milled to a cylindrical charge 250mm long and 38mm or 40.1mm in diameter depending on the weight of the charge. A 20.4g PETN booster and an Exploding Bridge Wire (EBW) detonator completed the setup. The accepted VoD of this diameter of Composition B will be 7800 m/s with a variation of 2%. The variability is due to slight differences in the exact composition during manufacture as well as changes in the composition as a result of extended storage.

5.2 Curve Fitting

The responses from the optical devices under test showed a gradual increase in the intensity of light as the shockwave approached the sensors. This effect had not been noted in the work of [3]. It can be explained by the attenuated transmission of light ahead of the shock front through a semi opaque material. The Beer-Lambert law [1] governs this attenuation and states,

$$I_{\text{through material}} \propto e^{-\text{distance travel through material}} \quad (3)$$

Hence if the hypothesis is true, an exponential curve should be able to be fitted to the rising edge. However this exponential fit does not persist due to the slew rate limiting of the op amps. That is, the rising edge may be better fit by a linear curve. This can be seen in Fig. 6. All falling edges look distinctly linear and can be attributed to slew rate limiting. Curve fitting is used to extrapolate the truncated peaks so that an average VoD can be calculated from non-deal data.

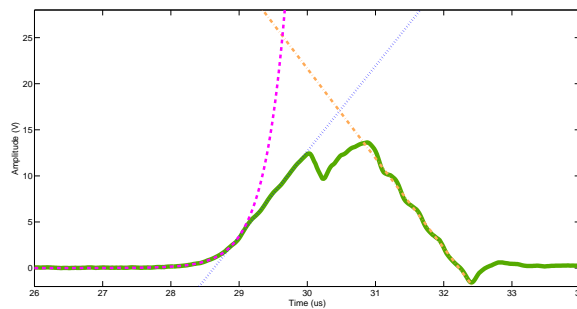


Figure 6: An exponential curve and a linear curve have been fitted to the rising edge of this pulse. It shows that the exponential curve is a good fit until the slew rate limit of the opamp is reached, after which a linear curve is a better fit.

5.3 Noise Peaks in PVDF

The responses from the PVDF contained considerable noise, some of which were common to all channels from the sensor array. An example of a response from one channel of a two sensor PVDF prototype is shown to demonstrate these features (Fig. 7). The main features that can be seen are:

- *EBW Discharge Current*: The start of a detonation is initiated by a signal ($t=0$) sent to the EBW firing unit. This initiation pulse when detected by the firing unit discharges a very high voltage and large current 2 us later. The measurement equipment measurement oscilloscope picks up EM interference generated by this
- *EBW vaporisation*: The first peak is due to the vaporisation of the bridgewire generating EM interference. As the EBW bridgewire breaks, it marks the start of a detonation as secondary explosive part of the EBW detonator starts reacting. This interpretation is supported by light starting to be detected at 8-12 us by fibre optic sensors being tested at the same time.
- *Unidentified common interference*: It is uncertain what these peaks are due to, however they appeared on all channels. These peaks cannot be attributed to the shock breakout from the detonator as this should occur on the order of 4 to 5 us after the bursting of the bridgewire [14]
- *Sensor Signal*: As the detonation front moves down the length of an explosive, it triggers each sensor to generate an output pulse progressively. The peak seen in the output graph (Fig. 7) is attributed to the response from the top sensor as it is first significant peak which is not common to the channels from both sensors. Furthermore it appears at approximately the right time, though this is very rough as it presumes the detonation front travels at the expected VoD throughout the detonation.
- *Line induction*: After the shock wave has passed over the sensors, eventually destroying them in the process, the coaxial signal line will no longer be terminated. These unterminated lines will act as antennas, picking up noise as the detonation and explosion continues

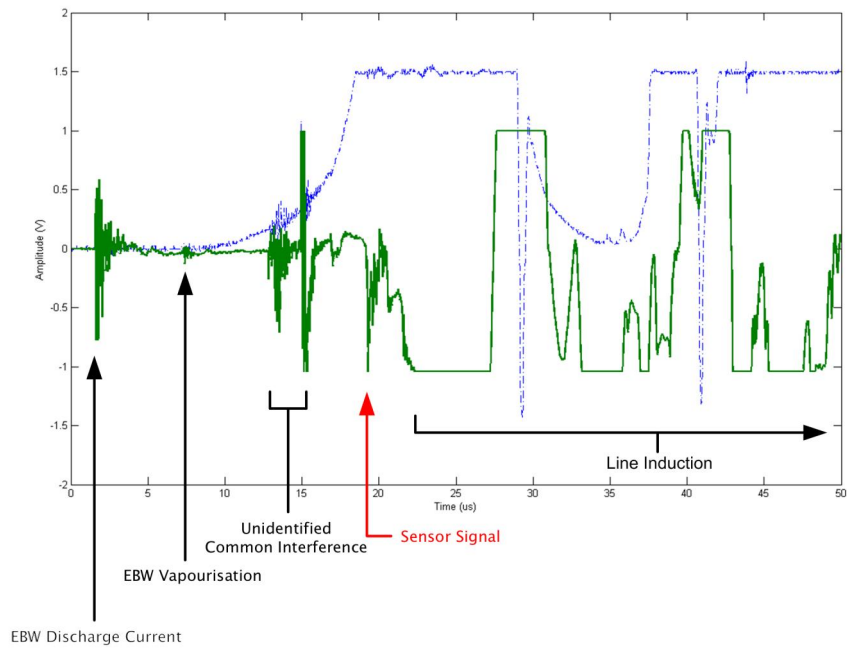


Figure 7: An example of the output signal (heavy line) produced from the top sensor of a double sensor piezo prototype. The suspected main events are identified on the diagram and explained above. The dash dotted line shows the response from an optical fibre perpendicular prototype which had been attached to the explosive at the same time.

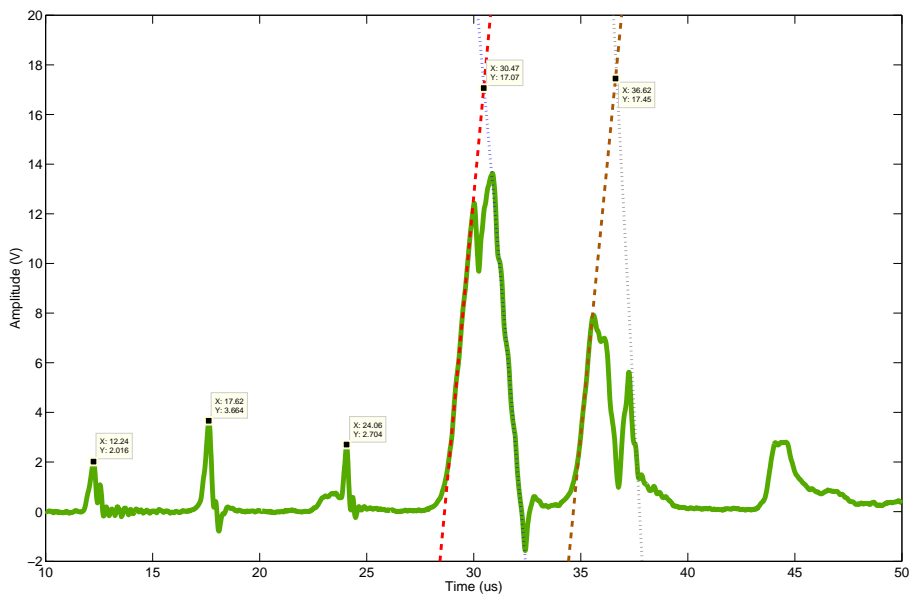


Figure 8: An example of the response from a four sensor FOP. Based on the known VoD of the explosive under test, the first peak can be confirmed to not have come from the first sensor. Instead the following four peaks are the response from the four sensors of the device. The separation distance between sensors was 50 mm and based on the time of each peak the average VoD can be calculated.

5.4 VoD Calculations

The average VoD for various prototypes and tests are summarised in Fig. 9. The data shows that using full peaks the FOP can achieve good results. Using curve fitted peaks though to calculate VoD for the optical responses gave variable, but similar to expected results. The perpendicular prototype shows promise, however the data was heavily truncated. The design was tested with a thinner fibre to reduce the amount of light reaching the photo-diode, but at the current sensitivity of the circuit it gave zero output. The results from the PVDF prototypes show that it is capable of accurate measurement of VoD, however it does not yet have the consistency desired.

Estimate Number	VoD		
	FOP (m/s)	Perpendicular (m/s)	PVDF
1	6500 CF	7900 CF	7800
2	7700		7800
3	7800		7600
4	7800		8200
5	7800 CF		
6	8000 CF		
7	8100 CF		

Figure 9: Summary of Average VoD. CF denotes that curve fitted data was used to calculate the VoD

5.5 Cost Analysis

In these experiments a limited number of sensors per device were manufactured to save time and cost. In a full device, 10 sensors would be required. Scaling of the estimated costs of the sensor arrays show that the replacement cost would be \$110 for the perpendicularly mounted PMMA fibres, \$81 for the FOP and \$60 for the PVDF sensors. These estimated costs are higher than what might be achieved if they were mass manufactured. Labour hours should significantly decrease while materials cost may marginally decrease under these conditions.

5.6 Usability

Based on usage during these experiments, the FOP is very easy to setup with few parts and few connections to make. It is also quite durable and takes little space in storage. The perpendicularly mounted fibres are equally easy to mount on the charge, however require a greater number of connections to be made to the circuit. The connection between the fibre and the pipe segment can break under rough handling. It is also quite bulky. The PVDF-based device is also quite durable and compact however the soldered wire joins between the PCB and Vero board are prone to failure. As with the perpendicularly mounted fibres, the separate channels used for each sensor result in the need for a large number of connections to be made which can be very time consuming. Thus the FOP seems the best in regards to human usability as a quick, robust and easy to use measurement device.

6. CONCLUSION

Both the FOP and PVDF prototypes show the greatest promise as a cheaper alternative to using piezoelectric pins for measuring VoD. For the FOP, the accuracy desired is achievable if full peaks from all sensors can be obtained. The form shown here is close to being fully usable, however greater work needs to go towards manufacturing the cavities more consistently and using smaller diameters to reduce the likelihood of saturation.

The PVDF prototype was able to detect peaks at times corresponding to the known sensors positions. However the responses showed considerable noise which can hamper the identification of the correct peaks from which to calculate VoD. Further investigations are needed into designs to minimise this noise, or else determine a way to remove some of the noise based on commonality between different channels. Once there is a better understanding of the effects which can degrade the response of these sensors, the PVDF could be packaged in its originally envisioned form as a flexible plastic sheet onto which several PVDF sensors have been manufactured and wired. The slim form-factor afforded by

such an implementation as well as the current form the FOP suggest that both of these methods could be used in situations not previously possible with piezoelectric pins, like cased charges.

7. ACKNOWLEDGEMENTS

The work was supported by the Explosives Group, Weapons Systems Division, DSTO. The assistance of the various staff at the DSTO is gratefully acknowledged, particularly Phil Davies and Mark Milnes. The critique and ideas of our supervisor Sam Mickan were of immense benefit. As were the guidance and experience of the workshop staff, particularly Ian Linke in the School of Electrical and Electronic Engineering at the University of Adelaide

REFERENCES

1. *Beer-Lambert Law*. Wikipedia [Online]. Available: http://en.wikipedia.org/wiki/Beer-Lambert_law. Accessed: 2004/09/15.
2. *Blackbody Radiation*. Electro Optical Industries Inc [Online]. Available: http://www.electro-optical.com/bb_rad/bb_rad.htm. Accessed: 2004/09/22.
3. *Blackbody Radiation*. Available: http://www.electro-optical.com/bb_rad/bb_rad.htm. Accessed: 2004/09/22.
4. *Fiber Optic Probe, development and optimisation*. TNO Prins Maurits Laboratory [Online]. Available: <http://www.pml.tno.nl/en/em/fop.html>. Accessed: 10/03/2004.
5. *Military Explosives*. Federation of American Scientists [Online]. Available: <http://www.fas.org/man/dod-101/navy/docs/fun/part12.htm>. Accessed: 2004/09/27.
6. Bauer, F., *PVDF Shock Sensors: Application to polar materials and high explosive*. IEEE Transactions on Ultrasonics, Ferroelectrics and Frequency Control, 2000. **47**(6): p. 1448 - 1454.
7. Davies, P., *Metallised Explosives*, E. Chan, Recipient. 2004/06/02, Adelaide.
8. Franco, S., *Design with Operational Amplifiers and Analog Integrated Circuits*. 3 ed. 2002, New York: McGraw-Hill.
9. Greene, E.F. and J.P. Toennies, *Chemical Reactions in Shock Waves*. 1966, London: Edward Arnold.
10. Held, M. and P. Nikowitsch. *Multi stage fibre optic probes*. in *16th International Congress on High Speed Photography and Photonics*. 1984. Strashbourg, France: The International Society for Optical Engineering (SPIE).
11. Lind, T. *Piezoelectricity*. [Online]. Available: <http://www.tedlind.net/Piezoelectricity.htm>. Accessed: 26th Sept.
12. Maynard, P. *Fire and Explosion Investigation: Section 2: Physics of Fires and Explosions*. [Online]. Available: <http://www.forensics.edu.au/downloads/Section2Physics.pdf>. Accessed: 13/03/2004.
13. Pattison, G., M. Keith, and A. Gregory. *Blackbody Radiation*. Eggescliffe School [Online]. Available: <http://www.eggescliffe.org.uk/physics/astronomy/blackbody/bbody.html>. Accessed: 2004/9/22.
14. RISI. *Technical Discussion of Exploding Bridgewire (EBW) Detonators*. risi-usa [Online]. Available: <http://www.risi-usa.com/0products/8td/page04.html>. Accessed: 2004/09/15.
15. Tulis, A.J. and J.R. Selman, *Characterization of shock and reactions fronts in detonations*. Review of Scientific Instruments, 1982. **53**: p. 1586-91.